BACHELOR

Influences of temperature and flow on MCRS measurements on an atmospheric-pressure jet

Bolk, Isabella

Award date:
2019

Eindhoven University of Technology

Department of Applied Physics

Bachelor Final Project

3CEX0

Influences of temperature and flow on MCRS measurements on an atmospheric-pressure jet

Author:
Isabella Bolk

Student number:
0994187

Supervisors:
ir. Bart Platier
ir. Tim Staps
dr.ir. Job Beckers

July 1, 2019

Abstract

The resolution of the plasma properties determined with the Microwave Cavity Resonance Spectroscopy technique has been improved over the years. With a pulsed RF atmospheric pressure plasma jet a plasma can be created that enters a cylindrical cavity and with the MCRS technique the shift in resonance frequency and the shift in reciprocal quality factor due to the plasma can be determined with a higher resolution than in the past. With a higher resolution, however, other influences that could be neglected before, now become important. In this research multiple influences on the resonance frequency and the quality factor of a cylindrical cavity are investigated. With the knowledge of the non-plasma influences on the resonance frequency and the quality factor, the plasma properties can be determined more accurately.

First the influence of the cavity temperature on the resonance frequency and the quality factor is studied by performing an MCRS measurement for different cavity temperatures. The results show that the resonance frequency changes with -73 ± 2 kHz per Kelvin increase in cavity temperature and that the quality factor decreases with increasing cavity temperature.

Secondly, the influence of the gas temperature on the cavity temperature is investigated by measuring the change in cavity temperature for different gas temperatures. For gas temperatures between 120 and 180 K, the change in cavity temperature per pulse is in the order of 10 μK for the theoretical model and in the order of μK for the measurements. It is predicted that in the gas temperature range of 400 to 1000 K, which is the temperature range that the creation of a plasma can cause, the change in resonance frequency after one pulse is between 1 Hz and 10 Hz for a pulse of 0.01 s. Moreover lowering the duty cycle lowers the influence that the gas temperature has on the cavity temperature for a constant pulse.

Lastly, the influence of the helium gas flow on the resonance frequency is studied by performing an MCRS measurement with and without a gas flow. Without the gas flow a 1 kHz noise in resonance frequency is measured and with the helium gas flow a 70 kHz noise is measured. The 70 kHz noise with a gas flow can be explained by a fluctuation in the gas composition of 3.8%. According to the prediction model, pressure changes in the order of 1 mbar can cause a noise in the order of 100 Hz. This is, however, for a cavity with only helium gas and therefore the influence of pressure changes on the resonance frequency should experimentally be determined.

Contents

Chapter 1

Introduction

In the past low pressure plasmas were the most common plasmas and were used for applications in for example materials processing [1]. However, these plasmas had to be created in an expensive vacuum environment and therefore it has been investigated how plasmas could be created at atmospheric pressure [2]. To determine properties of these plasmas the Microwave Cavity Resonance Spectroscopy (MCRS) technique is used. A cavity has certain resonance frequencies with corresponding quality factors. With the MCRS technique the initial resonance frequencies and quality factors are compared to the resonance frequencies and quality factors after a plasma is introduced inside the cavity. With the shift in resonance frequency and reciprocal shift in quality factor plasma properties, such as the electron density and the collision frequency, can be determined. In the past this shift in resonance frequency was in the order of MHz and had a resolution of 100 kHz. The reciprocal shift in quality factor was for this case not required. At the moment a radio frequency (RF) atmospheric pressure plasma jet is used to create a plasma that has a shift in resonance frequency in the order of 1 kHz and a resolution of 10 Hz. In this case the reciprocal shift in quality factor does influence the plasma properties that can be obtained with the MCRS technique. Since the resolution of the resonance frequency has been improved from the order of 100 kHz to 10 Hz, other influences on the resonance frequency become more important now. If a factor influenced the measured resonance frequency in the order of 1 kHz in the past, this was not visible in the derived values for the plasma properties. Now, however, the measured resonance frequency needs to be corrected for this influence to obtain reliable values for the plasma properties.

In this research a few possible influences on the resonance frequency and the quality factor are investigated. First the influence of the cavity temperature on the resonance frequency and the quality factor is determined by performing an MCRS measurement for different cavity temperatures. Secondly, the influence of the gas temperature on the cavity temperature is investigated by measuring the cavity temperature over time for different gas temperatures. Lastly, the influence of the helium gas flow is investigated by performing an MCRS measurement on the cavity with and without the gas flow.

In Chapter 2 the theory of MCRS is explained. The methods of the experiments are explained in Chapter 3, that includes a detailed description of the general setup, the method for the cavity temperature influence experiment, the method for the gas temperature influence experiment and the calibration of the temperature sensors. In Chapter 4 the results of the experiments are presented and discussed. Then a conclusion is given in Chapter 5.

Chapter 2

Theory

In this chapter the theory necessary for understanding the setup and the measurements is explained. Section 2.1 discusses the Microwave Cavity Resonance Spectroscopy technique.

2.1 MCRS

Microwave Cavity Resonance Spectroscopy (MCRS) is a plasma diagnostic method in which changes in the resonance behaviour are related to the electron dynamics of a plasma [3]. Every excited mode inside a cavity has a certain resonance frequency. This resonance frequency depends on the properties of the cavity, the medium inside the cavity and the environment to which the cavity is exposed. Examples of these properties are the permittivity of the gas and the cavity volume. When a plasma enters the cavity the permittivity of the medium is altered by the electrons in the plasma, which in turn alters the resonance frequency. The MCRS technique determines the shift in the resonance frequency. MCRS has, however, a detection limit, which depends on the quality factor, Q. The quality factor is related to the Full-Width-Half-Maximum (FWHM) of the resonance frequency peak. A higher quality factor leads to a smaller peak and therefore a lower detection limit. Small deviations in the resonance frequency can then be measured more precisely. However a high quality factor also leads to a poor temporal resolution. Therefore a trade-off needs to be made between an as low as possible detection limit and an as high as possible temporal resolution. By combining the shifts in resonance frequency and quality factor the electron density of the plasma can be determined. For this purpose cavity perturbation theory is used and the following equation is derived by van der Schans *et al.* [4]

$$\frac{\Delta f}{f_0} + \frac{i}{2}\Delta(\frac{1}{Q}) = -\frac{\iiint_{V_{cav}} \Delta\tilde{\varepsilon}|\mathbf{E_1}|^2 d^3\mathbf{r}}{2\varepsilon_0 \iiint_{V_{cav}} |\mathbf{E_1}|^2 d^3\mathbf{r}}, \tag{2.1}$$

where Δf is the shift in resonance frequency, f_0 the resonance frequency without plasma, $\Delta(\frac{1}{Q})$ the change in reciprocal quality factor, ε_0 the vacuum permittivity, V_{cav} the cavity volume, $\Delta\tilde{\epsilon}$ the change in complex permittivity and $\mathbf{E_1}$ the unperturbed electric field in the cavity.

The shift in complex permittivity of the medium inside the cavity compared to the complex permittivity without plasma is given by [4]

$$\Delta\tilde{\varepsilon} = -\frac{i\tilde{\sigma}}{\omega}, \tag{2.2}$$

where $\tilde{\sigma}$ is the complex plasma conductivity and ω the angular frequency of the time-harmonic electric field.

The complex plasma conductivity can be derived using kinetic theory and the following equation is obtained [4]

$$\tilde{\sigma} = \varepsilon_0 \frac{\omega_{pe}^2}{(\nu_{eff}^2 + \omega^2)}(\nu_{eff} - i\omega), \tag{2.3}$$

where ω_{pe} is the plasma electron frequency and ν_{eff} the effective collision frequency.

The plasma electron frequency is given by

$$\omega_{\mathrm{pe}} = \sqrt{\frac{n_{\mathrm{e}} e^2}{\varepsilon_0 m_{\mathrm{e}}}}, \tag{2.4}$$

where n_e is the electron density, e the elementary charge and m_{e} the mass of an electron.

When Equations 2.2 and 2.3 are combined, the following equation for the change in complex permittivity is obtained

$$\Delta\tilde{\varepsilon} = -\varepsilon_0 \left(\frac{\omega_{pe}^2}{(\nu_{eff}^2 + \omega^2)} + \frac{i\nu_{eff}}{\omega} \frac{\omega_{pe}^2}{(\nu_{eff}^2 + \omega^2)} \right). \tag{2.5}$$

After substituting Equation 2.5 in Equation 2.1, two equations for the shift in resonance frequency and the shift in reciprocal quality factor are obtained by separating the real and imaginary parts. The shift in resonance frequency is given by

$$\frac{\Delta f}{f_0} = \frac{1}{2} \frac{\omega_{pe}^2}{(\omega_0^2 + \nu_{eff}^2)} \mathcal{V}, \tag{2.6}$$

where $\mathcal{V}$ is the ratio of the effective plasma volume and the effective cavity volume. The change in reciprocal quality factor is given by

$$\Delta\left(\frac{1}{Q}\right) = \frac{\nu_{eff}}{\omega_0} \frac{\omega_{pe}^2}{(\omega_0^2 + \nu_{eff}^2)} \mathcal{V}. \tag{2.7}$$

The ratio of the effective plasma volume and the effective cavity volume is given by

$$\mathcal{V} = \frac{\iiint_{V_p} |\mathbf{E_1}|^2 d^3\mathbf{r}}{\iiint_{V_{cav}} |\mathbf{E_1}|^2 d^3\mathbf{r}}, \tag{2.8}$$

where V_p is the plasma volume.

By combining Equations 2.6 and 2.7 the following equation is obtained for the effective collision frequency

$$\nu_{eff} = \pi f_0 \frac{\Delta(\frac{1}{Q})}{\frac{\Delta f}{f_0}}. \tag{2.9}$$

An equation for the electron density is obtained by combining Equations 2.4 and 2.6 and is given by

$$n_e = \frac{2\varepsilon_0 m_e}{e^2} \frac{(\nu_{eff}^2 + 4\pi^2 f_0^2)}{\mathcal{V}} \frac{\Delta f}{f_0}. \tag{2.10}$$

Chapter 3

Method

In this chapter the setup and methods for the measurements are explained. In Section 3.1 the general setup that is used for MCRS measurements on a radio-frequency jet is explained. Then the experiment that investigates the influence of the cavity temperature on the resonance frequency and the quality factor is explained in Section 3.2. In Section 3.3 the method of the experiment investigating the influence of the gas temperature on the cavity temperature is explained. The calibration of the temperature sensors is given in Section 3.4.

3.1 General setup

The general setup that is used in this research is shown in Figure 3.1. The plasma source is a plasma jet that produces radio frequency driven plasma pulses. The plasma jet consists of a polycarbonate housing with a feed gas inlet on top, where helium gas flows into the system at a volumetric rate of 1 slm. The gas then flows into a quartz tube that has a 1 mm inner radius and 2 mm outer radius. Inside this tube there is a needle electrode made of tungsten with a radius of 0.5 mm and a tip angle of around 20°. The pulses are created by a pulse/delay generator (BNC model 575), that outputs a block wave with a peak to peak voltage of 5 V and a minimum voltage of 0 V. These pulses are send to a function generator that outputs a block wave with a peak to peak voltage of 10 V with a minimum of -5 V and a certain maximum peak time given as input. The signal is then send to a second function generator (Agilent 33220a) that creates a sine wave with an adjustable peak to peak voltage that has a maximum of 600 mV. When the signal of the first function generator is at 5 V, the second function generator reaches the maximum voltage and when it is at -5 V the second function generator returns 0 V. Then an amplifier (Amplifier Research) is connected to the second function generator that amplifies the peak to peak voltage of the signal. To have an optimum transition of power from the amplifier to the load the impedance of both devices should be equal. To obtain this a match box is placed between the amplifier and the plasma jet that controls the impedance of the plasma jet and the match box combined. Then the pulse reaches the needle electrode. The voltage on the needle is measured with a voltage probe that is connected to a screw that reaches the inside of the plasma jet. The current towards the needle electrode is measured with a Rogowski coil. The plasma jet is placed coaxially with a cylindrical microwave cavity that is used as a ground electrode. The cavity has an inner radius of 33 mm and an inner length of 16 mm. The outer radius is 36 mm and the outer length is 26 mm. The cavity is made of aluminium and has two similar circular holes in the middle of the flat sides with a radius of 6.5 mm, where the gas and the plasma can flow in and out of the cavity. A Keysight E5063A ENA Series Network Analyzer with a range of 100 kHz up to 8.5 GHz is connected to the cavity to perform the MCRS. In this experiment two temperature sensors are used that are connected to the cavity wall. Each of the sensors is connected to an Agilent 34410A 6 1/2 Digit Multimeter that reads the voltage

of the temperature sensors. The temperature sensors are calibrated before the experiments and the results of the calibration are presented in Section 3.4.

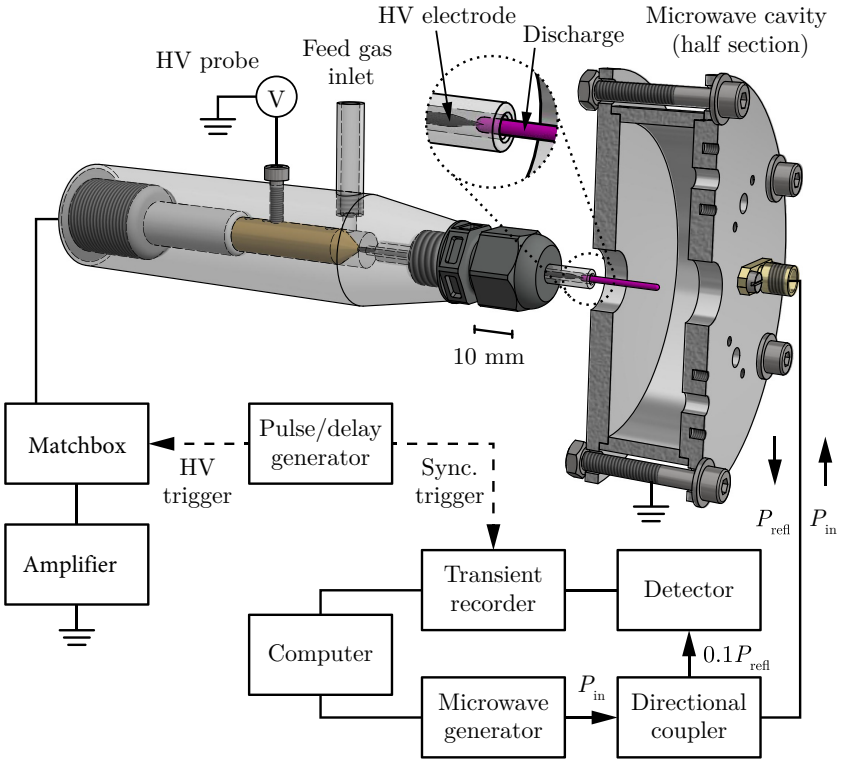

Figure 3.1: The general setup used in the measurements [4].

3.2 Method cavity temperature influence

The influence of the cavity temperature on the resonance frequency and the quality factor is investigated by performing an MCRS measurement for different cavity temperatures. For this purpose a temperature calibration device of the Coherence and Quantum Technology faculty at Eindhoven University of Technology is used. The device consists of a box in which the cavity with temperature sensors attached can be placed. The cooling inside the box is constant and the heating element regulates the temperature of the box that can be adjusted up till the order of 0.1 °C. For temperatures below 28 °C the device has difficulty establishing thermal equilibrium. Therefore for these temperatures the box has to be opened slightly to provide extra cooling at a temperature of around 23 °C. The cylindrical cavity of the setup as described in Section 3.1 is placed without the plasma jet inside the temperature calibration device with the temperature sensors and the network analyzer connected to the cavity wall. The setup can be seen in Figure 3.2. The temperature range that is used in this experiment is from 23 °C to 35 °C. At every temperature the MCRS measurement is performed 250 times for both the TM_{010} and the TM_{110} mode with an averaging factor of 16, which means that the network analyzer will actually measure the reflected power 16 times during each MCRS measurement and average the results. For this purpose two frequency ranges around the initial resonance frequencies are used with a width of 100 MHz each. The network analyzer is first calibrated to correct for the cable. The resonance frequency of the TM_{010} mode is at room temperature around $3.51 \cdot 10^9$ Hz and the resonance frequency of the TM_{110} mode is around $5.45 \cdot 10^9$ Hz [4]. The network analyzer returns the reflected power for 1401 measurement points inside the frequency range of both modes at every one of the 250 measurements. The measured data is then processed using a script that finds the values for the resonance frequency and the quality factor for each of the 250 measurements by using a fit function.

Figure 3.2: The cavity inside the temperature calibration device.

3.3 Method gas temperature influence

To determine the influence of the gas temperature on the resonance frequency of the cavity, the temperature of the cavity is measured for different inlet gas temperatures. The temperature range of the inlet gas is chosen between 120 and 180 K with steps of 10 K. For this measurement the setup of Section 3.1 is used without the plasma jet. A Brooks mass flow controller is used to let helium gas into the heating device at a constant volumetric rate of 1 slm. A constant volumetric rate has been chosen to minimize pressure changes inside the cavity. A Controlled Evaporator Mixer (CEM) of the company Bronkhorst is used as a heating device to change the temperature of the helium gas. When the gas leaves the CEM, the helium flows into a tube that is isolated with aluminum foil to limit heat loss. Then the gas flows into a small glass tube with the same diameter as the tube in the plasma jet, which is placed a millimetre away from the opening of the cavity as can be seen in Figure 3.3. The temperature sensor is connected to the cavity and measures the temperature of the cavity every second. The network analyzer is also connected to the cavity and performs a measurement every second with an averaging factor of 16. For every gas temperature a 30 minutes measurement is performed. During the measurement the lab temperature is also measured with a KlimaLogg Pro device that registered the temperature up till the order of 0.1 °C every minute.

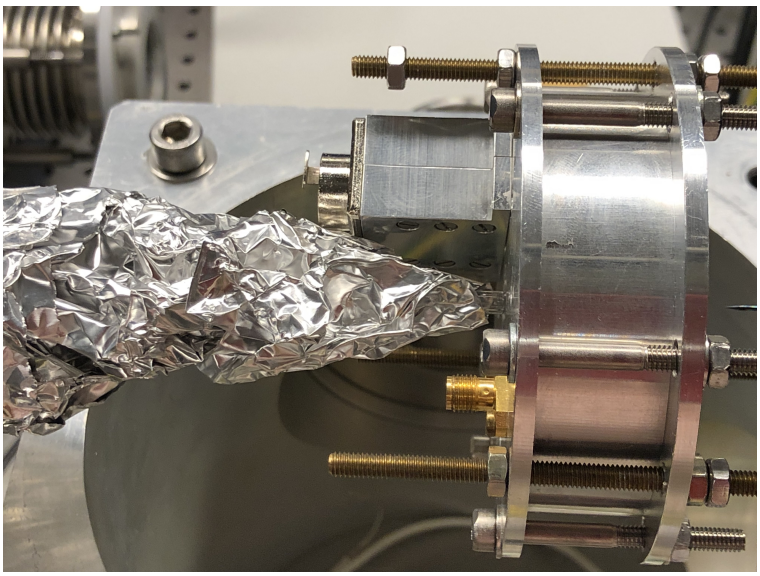

Figure 3.3: A close-up of the inlet gas tube and the cavity.

3.4 Calibration of temperature sensors

The temperature sensors that are used during the experiments need to be calibrated. For this purpose the setup described in Section 3.2 is used. The temperature range that is used to calibrate the sensors is from 23 °C to 35 °C. At every temperature the output voltage of the temperature sensors is measured 250 times.

The results of the calibration of both temperature sensors is presented in Figure 3.4. For temperature sensor 1 the correct settings are 86.9 ± 0.8 mV K^{-1} with an intercept of 0.32 ± 0.02 V. For temperature sensor 2 the correct settings are 86.8 ± 0.8 mV K^{-1} with an intercept of 0.31 ± 0.03 V. The sensor that is used in the experiment explained in Section 3.3 is referred to as temperature sensor 1.

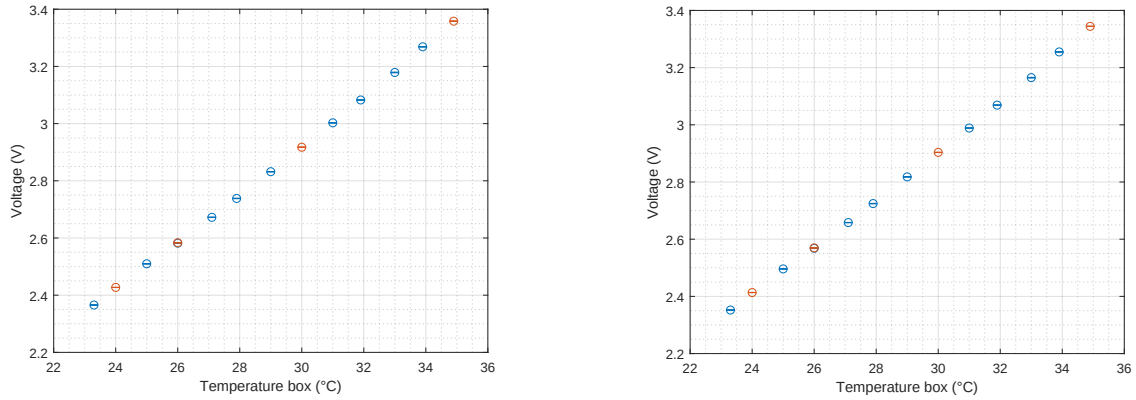

(a) The calibration of temperature sensor 1.

(b) The calibration of temperature sensor 2.

Figure 3.4: The calibration of the temperature sensors where the voltage is plotted against the temperature. The red and blue data points represent two different measurement days, where the red data points are measured on an earlier day.

Chapter 4

Results and discussion

In this chapter the results of the performed measurements are presented and discussed. In Section 4.1 the influence of the cavity temperature on the resonance frequency and the quality factor is discussed. Then the influence of the gas temperature on the cavity temperature is discussed in Section 4.2. Lastly, in Section 4.3 the influence of the helium gas flow on the resonance frequency is discussed.

4.1 Influence of the cavity temperature on the resonance frequency and the quality factor

When the temperature of the cavity increases the cavity will thermally expand. The resonance frequency will therefore decrease. The thermal expansion is approximated by the linear expansion equation since the expansion is in the order of μm. The linear thermal expansion equation is given by [5]

$$\Delta l = l_0 \alpha_{Al} \Delta T_{cav}, \tag{4.1}$$

where Δl is the change in length, l_0 the initial length, α_{Al} the linear thermal expansion coefficient of aluminum and ΔT_{cav} the change in cavity temperature compared to the initial cavity temperature. Equation 4.1 can be rewritten to represent the wavelength change of a standing wave inside the cavity and is given by

$$\Delta \lambda = \lambda_0 \alpha_{Al} \Delta T_{cav}, \tag{4.2}$$

where $\Delta\lambda$ is the change in wavelength and λ_0 the initial wavelength. By using Equation 4.2 and the fact that $\lambda = \frac{c}{f}$, the relation between the change in resonance frequency, Δf, and the change in temperature of the cavity is determined and given by

$$\frac{\Delta f}{f_0} = -\frac{\alpha_{Al} \Delta T_{cav}}{1 + \alpha_{Al} \Delta T_{cav}}, \tag{4.3}$$

where f_0 is the initial resonance frequency.

For the temperature range that is used in the experiment described in Section 3.2, the change in resonance frequency is calculated. The value that is used for the linear expansion coefficient of aluminum is equal to $24 \cdot 10^{-6}$ K^{-1} [5]. The results of this calculation are shown in Figure 4.1, which shows the shift in resonance frequency for different cavity temperatures.

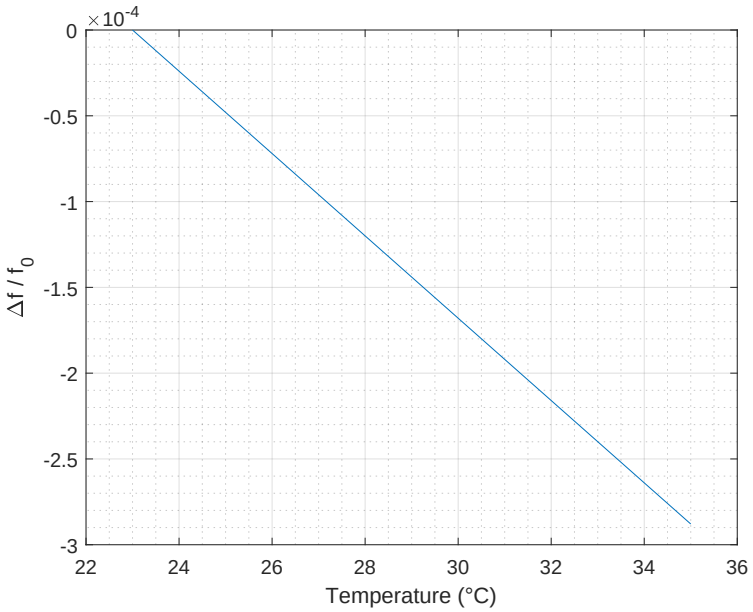

Figure 4.1: The expected $\Delta f/f_0$ for different cavity temperatures, where the reference temperature is 23 °C.

The measurement as described in Section 3.2 is performed. Typical results of MCRS measurements are shown in Figure 4.2, where the reflected power is plotted against the frequency for a cavity temperature of 23.3 °C and 27.9 °C. The TM_{010} mode is plotted in Figure 4.2a and the TM_{110} mode in Figure 4.2b. These figures show that while the resonance peak is shifted the shape of the peak remains almost the same for different temperatures.

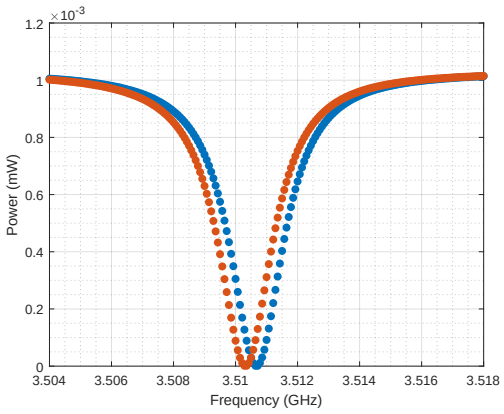

(a) The reflected power against the frequency for the TM_{010} mode.

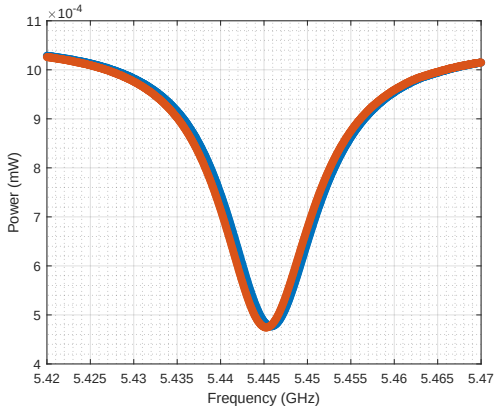

(b) The reflected power against the frequency for the TM_{110} mode.

Figure 4.2: The reflected power against the frequency for both modes. The blue line represents the power at a temperature of 23.3 °C and the red line the power at a temperature of 27.9 °C.

The values of the resonance frequency and the quality factor for different cavity temperatures that are determined in this experiment are shown in Figure 4.3 and Figure 4.4 respectively for both the TM_{010} and the TM_{110} mode. The shift in resonance frequency and the change in reciprocal quality factor are also shown in these figures.

In Figure 4.3 can be seen that the relation between the resonance frequency and the temperature is linear. For the TM_{010} mode the slope is -73 ± 2 kHz with an offset of 3512.36 ± 0.05 MHz

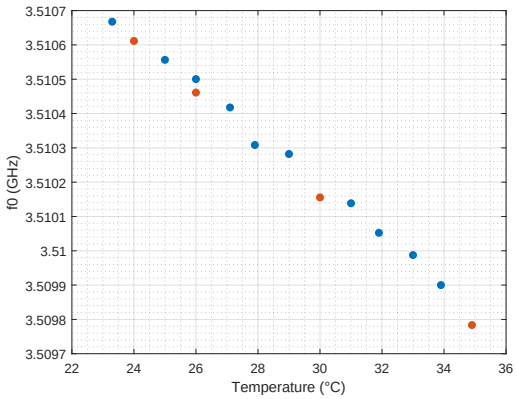

(a) The f_0 of the TM_{010} mode for different temperatures.

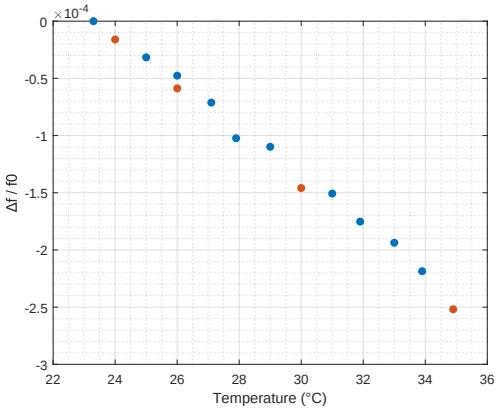

(b) The $\Delta f/f_0$ of the TM_{010} mode for different temperatures.

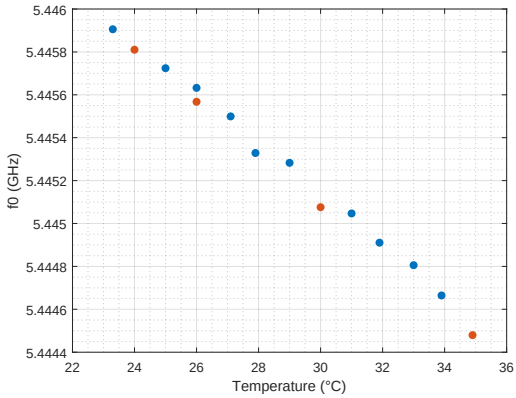

(c) The f_0 of the TM_{110} mode for different temperatures.

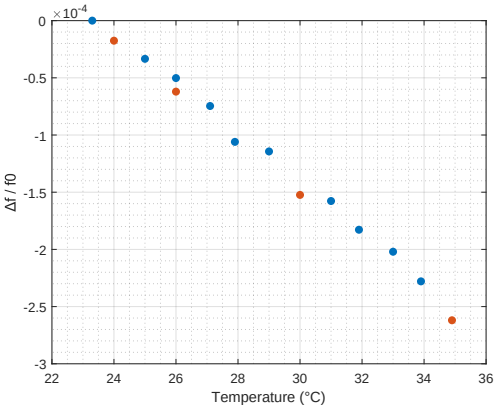

(d) The $\Delta f/f_0$ of the TM_{110} mode for different temperatures.

Figure 4.3: The resonance frequency and the shift in resonance frequency for different cavity temperatures and for both the TM_{010} and the TM_{110} mode. The red and blue data points represent two different measurement days, where the red data points are measured on an earlier day.

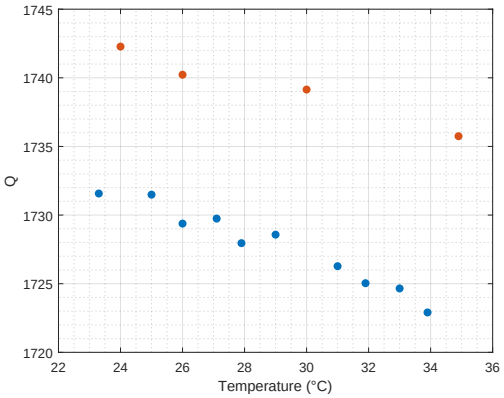

(a) The Q of the TM_{010} mode for different temperatures.

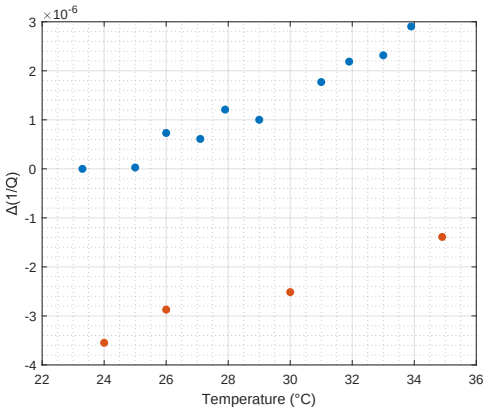

(b) The $\Delta(1/Q)$ of the TM_{010} mode for different temperatures.

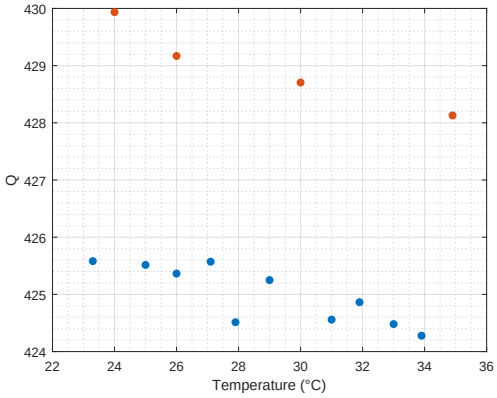

(c) The Q of the TM_{110} mode for different temperatures.

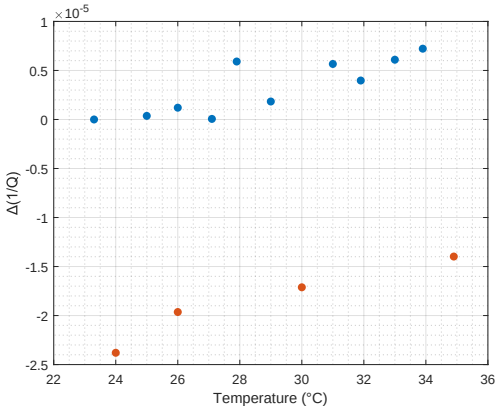

(d) The $\Delta(1/Q)$ of the TM_{110} mode for different temperatures.

Figure 4.4: The quality factor and the reciprocal shift in the quality factor for different cavity temperatures and for both the TM_{010} and the TM_{110} mode. The red and blue data points represent two different measurement days, where the red data points are measured on an earlier day.

and for the TM_{110} mode the slope is -120 ± 3 kHz with an offset of 5448.71 ± 0.09 MHz. The measurements are performed over a two day period and there is a discrepancy between the data from the two different days. The fact that the two modes have different values for the slope could be due to the fact that the quality factor and the depth of the peak of the TM_{110} mode are much lower then of the TM_{010} mode. Therefore the results of the TM_{010} mode are more reliable. In Figure 4.4 can be seen that the quality factor decreases with increasing cavity temperature. In this figure it is also clear that there is a significant discrepancy between the data from the two different days. The discrepancy between the two measurement days might be caused by a change of mechanical stress in the cavity. The discrepancy is more noticeable for the quality factor than for the resonance frequency and thus the quality factor is more sensitive to disturbances then the resonance frequency.

These graphs can be used to adjust the reference resonance frequency and quality factor for an experiment when the temperature of the cavity changes over time. In the current situation the shift in resonance frequency and reciprocal shift in quality factor is determined by comparing the measured resonance frequency and quality factor with the initial reference frequency and the initial quality factor that are determined at the initial temperature of the cavity. When the cavity temperature changes, however, the reference resonance frequency and quality factor also change. When the reference resonance frequency and quality factor are not corrected for the cavity temperature, this will lead to errors in the results when the temperature of the cavity changes.

In Figure 4.5 the theoretical and measured change in resonance frequency are compared as shown before in Figure 4.1 and 4.3b respectively. It can be seen that the decrease is of the same order. According to the experimental results the thermal expansion coefficient of the cavity is equal to $(20.7 \pm 0.4) \cdot 10^{-6}$ K^{-1} using Equation 4.3. This is slightly lower than $24 \cdot 10^{-6}$ K^{-1}, which is the theoretical value of the thermal expansion coefficient of aluminum [5]. This can be due to the fact that the cavity is not made of one piece of aluminum, but consists of separate aluminum components that are connected. For the calculation the linear expansion equation is used, while in reality the equation is more complex. This could be the reason for the slight deviation between the results. It is also possible that the deviation is due to an error in the temperature calibration device that was used for the calibration. Moreover, an error in the results of the temperature calibration can be the cause for a part of the deviation. The slope of Figure 3.4a is 86.9 ± 0.8 mV K^{-1} and therefore for the lowest possible slope of 86.1 mV K^{-1} the measured temperature of 35 °C in Figure 4.5 could be 0.3 °C lower at most. This could lead to a slightly higher value of the thermal expansion coefficient, but it would still be lower than the theoretical value.

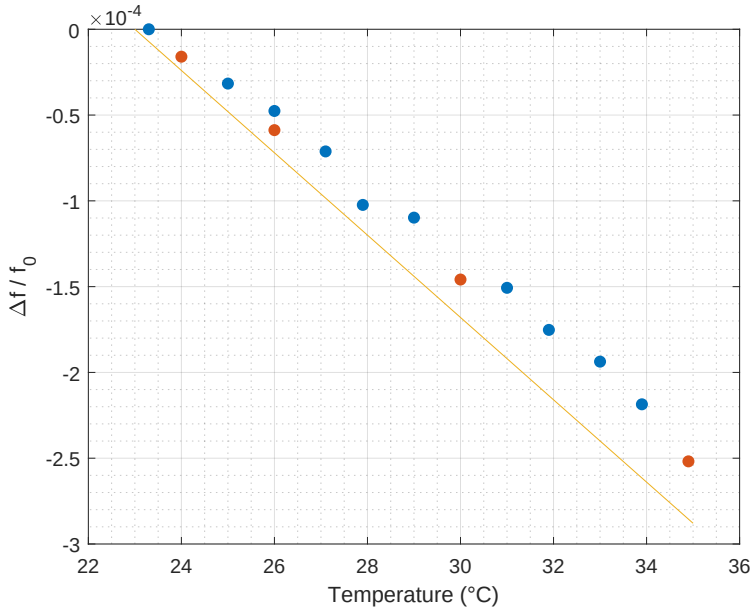

Figure 4.5: The expected and the measured $\Delta f/f_0$ for different cavity temperatures, where the reference temperature is 23 °C. The red and blue data points represent two different measurement days, where the red data points are measured on an earlier day.

4.2 Influence of the gas temperature on the cavity temperature

When the plasma is created inside the plasma jet, the helium gas surrounding the plasma is heated. This in turn influences the cavity temperature.

The conduction in a flow tube is approximated using the Penetration theory [6]. This theory is applicable when the following statement holds

$$\frac{\delta_h}{L} = \frac{2\sqrt{\pi a t}}{L} \leq 1, \tag{4.4}$$

where δ_h is the penetration depth, L the characteristic length of the cylinder, a the thermal diffusivity of helium gas and t the time.

In the radial direction of the flow tube the Penetration theory cannot be applied. In the axial direction, however, Equation 4.4 holds and is equal to 0.05 with $a = 1.9{\cdot}10^{-4}$ m^2 s^{-1}, $L = 30$ mm and $t = 1$ ms.

According to the Penetration theory the temperature function at a distance x is given by [6]

$$T(x,t) = (T_0 - T_1) \cdot \mathrm{erf}\left(\frac{x}{\sqrt{4at}}\right) + T_1, \tag{4.5}$$

where T_0 is the initial temperature of the gas inside the cavity, T_1 the temperature of the gas around the plasma just after the plasma is created, x the distance from the initial position of the plasma and T the temperature at position x and at time t.

For $x = 30$ mm and $t = 1$ ms the value of the error function is approximately 1, which indicates that the temperature of the gas inside the cavity will not change in the time of a pulse due to conduction.

To predict the influence of convection with respect to radial conduction the dimensionless Graetz number, G_z, is determined, which is defined as the ratio between the rate of heat transport due

to radial conduction and the heat transport due to axial convection [6]. The Graetz number is given by

$$G_z = \left(\frac{aL}{\langle v \rangle \, d^2} \right), \tag{4.6}$$

where $\langle v \rangle$ is the average flow velocity in the tube and d is the diameter of the tube.

The average flow velocity is given by

$$\langle v \rangle = \frac{Q_{He}}{\pi r^2}, \tag{4.7}$$

where Q_{He} the volumetric flow rate of the helium gas in $\mathrm{m}^3\ \mathrm{s}^{-1}$ and r the radius of the tube. For $d = 1$ mm, $Q_{He} = 0.0167 \cdot 10^{-3}\ \mathrm{m}^3\ \mathrm{s}^{-1}$, $r = 0.5$ mm and $L = 30$ mm the value of G_z is approximately 0.27, which indicates that the axial convection has a larger influence than the radial conduction.

An analysis is made to determine what the maximum change in temperature of the cavity wall is after one pulse due to axial convection. The energy necessary to heat up the helium gas to a certain gas temperature around a plasma in the time of one pulse, E_{He}, is given by

$$E_{He} = m_{He} C_{pHe} \Delta T_{He}, \tag{4.8}$$

where m_{He} is the mass of helium gas per pulse that flows inside the plasma jet, C_{pHe} the heat capacity of helium gas and ΔT_{He} the change in gas temperature due to the plasma.

The mass of helium gas that flows inside the plasma jet per pulse is given by

$$m_{He} = \rho_{He} Q_{He} t_{pulse} D, \tag{4.9}$$

where ρ_{He} is the density of helium gas, t_{pulse} the time of one pulse and D the duty cycle of the pulse.

The energy necessary to heat up the cavity with one degree, Q_{cav}, is given by

$$Q_{cav} = C_{pAl} m_{cav}, \tag{4.10}$$

where C_{pAl} is the heat capacity of aluminum and m_{cav} the mass of the cavity.

The maximum increase in cavity temperature due to the gas temperature is when all the energy that is used for heating the helium gas is also used for heating the cavity. This increase in temperature after one pulse, ΔT_{cav}, can be obtained from Equations 4.8 and 4.10 and is given by

$$\Delta T_{cav} = \frac{E_{He}}{Q_{cav}} = \frac{m_{He} C_{pHe} \Delta T_{He}}{C_{pAl} m_{cav}}. \tag{4.11}$$

The values of the different variables presented in this section are given in Table 4.1.

Table 4.1: The values of the different variables that are used for the calculation of the maximum change in cavity temperature due to convection.

Variables	Values
ρ_{He}	$0.1786\ \mathrm{kg\,m^{-3}}$ [7]
C_{pHe}	$5193\ \mathrm{J\,kg^{-1}\,K^{-1}}$ [7]
C_{pAl}	$897\ \mathrm{J\,kg^{-1}\,K^{-1}}$ [7]
Q_{He}	$0.0167 \cdot 10^{-3}\ \mathrm{m^3\,s^{-1}}$
m_{cav}	0.1 kg
t_{pulse}	0.01 s

The maximum change in temperature of the cavity is calculated for different changes in gas temperature and for different values of the duty cycle. The results are shown in Figure 4.6.

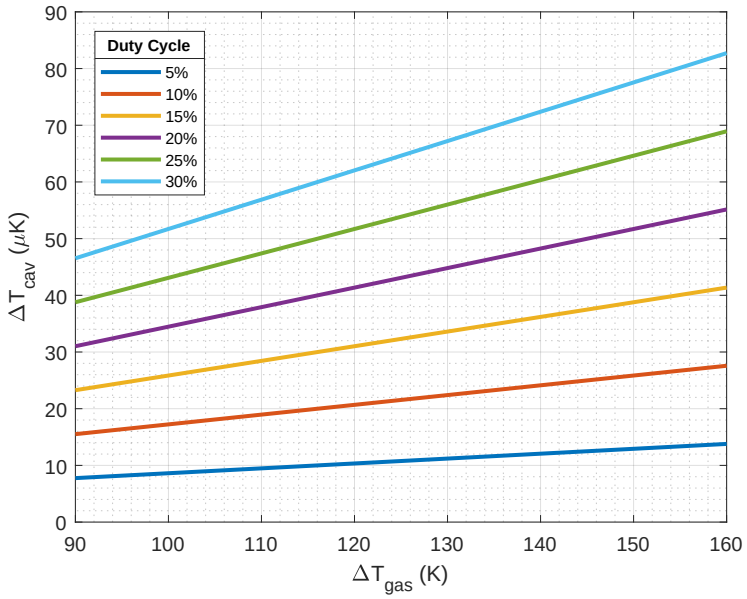

Figure 4.6: The temperature change of the cavity for different gas temperatures changes. The different lines represent pulses with different duty cycles.

The measurement as described in Section 3.3 is performed to experimentally determine the change in cavity temperature for different gas temperature changes.

In Figure 4.7 the change in cavity temperature is shown over time for different gas temperatures. The temperature change of the lab is used to analyze these graphs. For $T_{gas} = 140$ °C the lab temperature was 21.8 °C at $t = 0$ s and the initial cavity temperature was 22.5 °C. This means that the cavity will warm up slower than in the case where the cavity temperature had completely cooled down to the lab temperature. For $T_{gas} = 120$ °C the lab temperature was 22.7 °C at $t = 0$ s and the initial cavity temperature was 22.4 °C. In this case the lab will warm up the cavity along with the heated gas. This means that the measured increase in temperature is higher than in the case where the initial cavity temperature and lab temperature are equal. The temperature difference is due to the fact that the gas temperature of helium without heating is lower than the lab temperature and the gas flow had cooled down the cavity before the heating device was activated. For the other gas temperatures the cavity temperature is equal to the lab temperature at $t = 0$ s. For $T_{gas} = 120$ °C and $T_{gas} = 140$ °C the lab temperature remained stable during the measurement. For all the other gas temperatures the lab temperature slowly decreased with approximately 0.5 °C in one measurement. Therefore the slope will decrease over time in Figure 4.7.

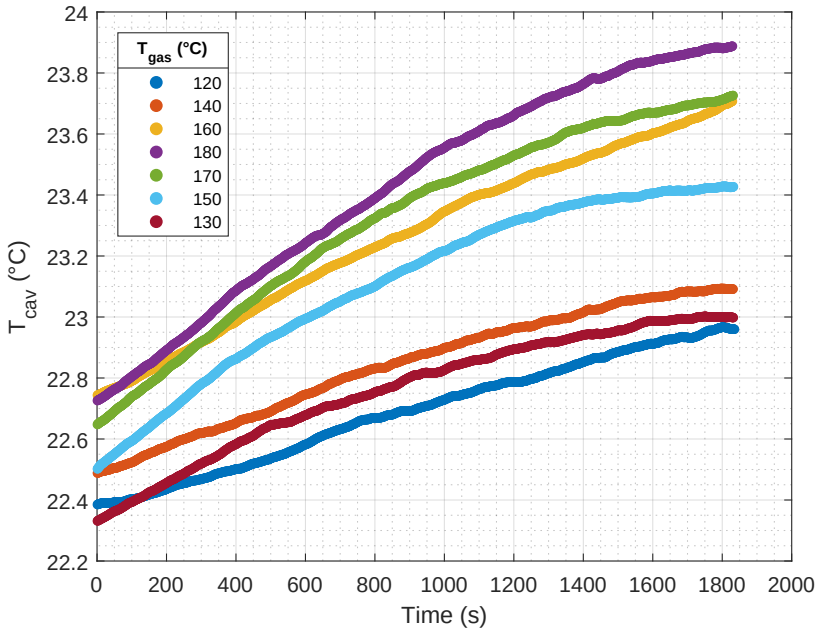

Figure 4.7: The temperature change of the cavity for different gas temperatures over time.

To determine the change in cavity temperature per minute, a second degree polynomial is fitted for every gas temperature in Figure 4.7. In Appendix A the graphs with the fits are shown separately for every gas temperature. The slope of every fit is averaged from $t = 400$ s to $t = 1300$ s to exclude the non-linear behavior that is due to lab temperature changes as much as possible. The average slope is used to calculate the change in cavity temperature per minute. In Figure 4.8 the change in cavity temperature per minute is plotted against the change in gas temperature. The expected deviation for $T_{gas} = 140$ °C is clearly visible in this figure. Moreover in Figure 4.8 a linear fit through the data points is plotted with a slope of 0.36 mK increase in cavity temperature per minute per degree Kelvin increase of the change in gas temperature.

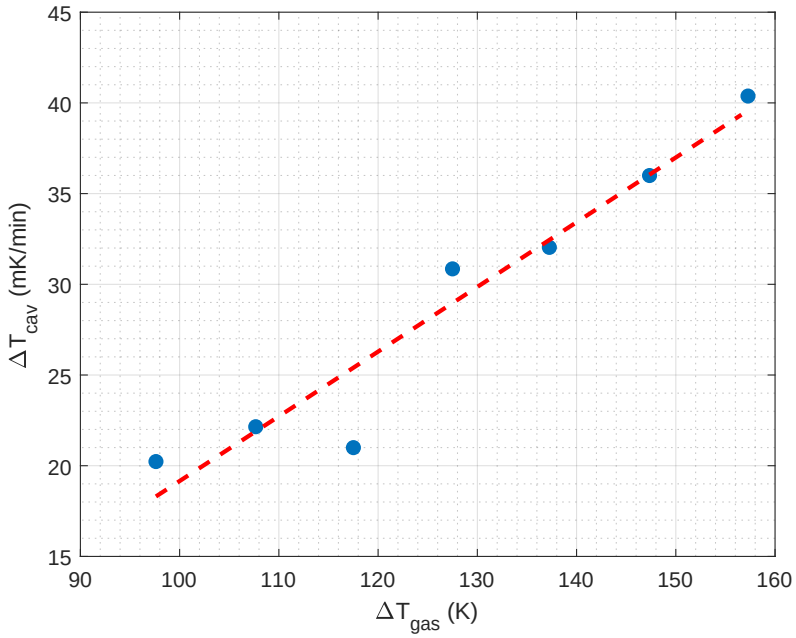

Figure 4.8: The temperature change of the cavity per minute for different gas temperatures changes.

To compare the experimental results with the expectation model, the change in cavity temperature per pulse is calculated for different duty cycles and is shown in Figure 4.9. For this purpose the data of Figure 4.8 is used to calculate the change in cavity temperature per pulse for $t_{pulse} = 0.01$ s and then these values are multiplied with different values for the duty cycle.

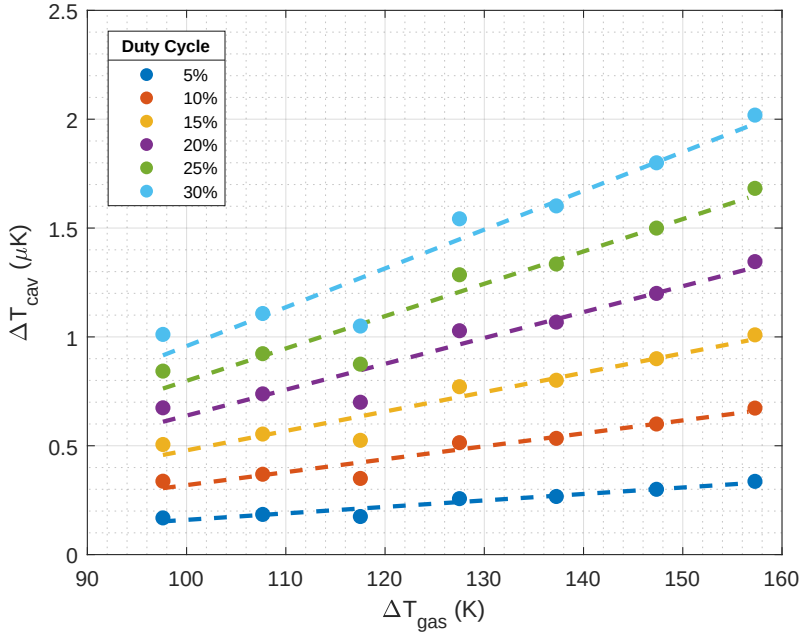

Figure 4.9: The temperature change of the cavity per pulse for different gas temperatures changes. The different lines represent pulses with different duty cycles.

According to the calculated maximum change in cavity temperature per pulse for different gas temperatures and for different duty cycles shown in Figure 4.6, the change in cavity temperature

is in the order of 10 μK. The measured change in cavity temperature shown in Figure 4.9 is in the order of μK. As expected the measured change is lower than the calculated maximum change since a part of the input energy is lost to the environment. From both the measured change and the calculated maximum change in cavity temperature, it can be concluded that a lower duty cycle leads to a smaller influence of the gas temperature on the cavity temperature.

The measured change in cavity temperature, however, does not correspond correctly with the according gas temperature changes, since the set temperature value on the heating device is not the same as the actual gas temperature that reaches the glass tube. Although the heat loss between the heating device and the glass tube is minimized using aluminum foil, there will still be some heat loss. Therefore the actual change in gas temperature is most likely lower than the values shown in Figure 4.9.

During the measurement the heating device might not only have heated the gas, but also the environment of the device including the cavity, the temperature sensor and the connected cables. This might have affected the measured cavity temperature. The cooling process of the device also took a long time period and therefore a fan was used to speed up this process. The room temperature was not stable during the measurements and although the change in room temperature was measured during all the measurements, it was hard to correct the obtained results since it is unknown how fast the change in room temperature affected the cavity temperature. Since the room temperature changed during the measurements it was also hard to have one initial cavity temperature for every measurement. Therefore it was decided to at least obtain an initial cavity temperature close to the room temperature at the start of every measurement. To improve the reliability of these measurements the experiment should be performed in a stable and controlled environment and with a more accurate heating device to make sure that the gas that enters the glass tube actually has the temperature given as input.

4.3 Influence of the helium gas flow on the resonance frequency

To measure the influence of the helium gas flow on the resonance frequency two measurements are performed using the setup as described in Section 3.3. For the first measurement an MCRS measurement is performed without a gas flow. The second measurement is with the helium gas flow, while the heating device is not used to heat the gas.

The results of the measurement without the gas flow are presented in Figure 4.10. As can be seen the noise is in the order of kHz.

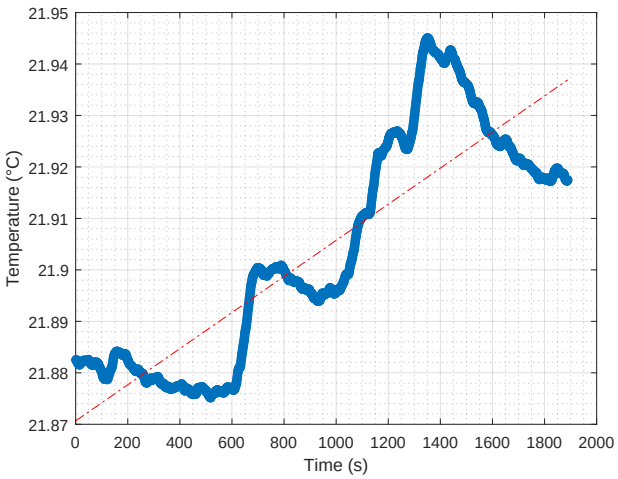

(a) The cavity temperature over time.

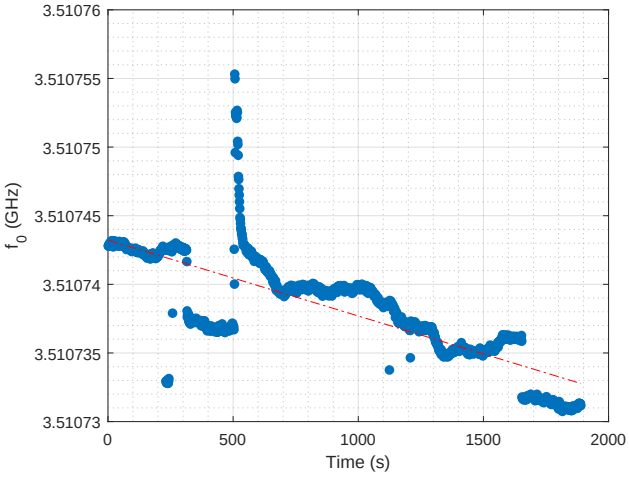

(b) The resonance frequency over time.

Figure 4.10: The cavity temperature and the resonance frequency over time without a gas flow.

In Figure 4.11 the results of the measurement with the helium gas flow are shown. The noise in this measurement is around 70 kHz. In the gas heating measurement the cavity temperature increased with approximately one degree Kelvin and according to the results of Section 4.1 the shift in resonance frequency would then also be around 70 kHz. This means that the shift in resonance frequency cannot be measured accurately enough with the network analyzer in this setup. Since the noise is higher with the helium gas flow than without, the 70 kHz noise is due to the flow.

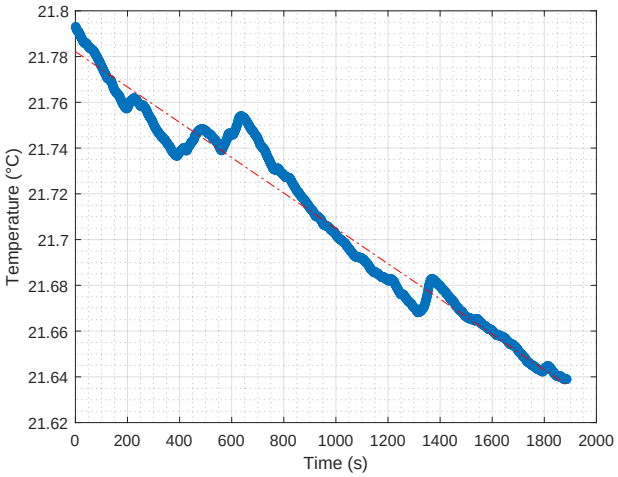

(a) The cavity temperature over time.

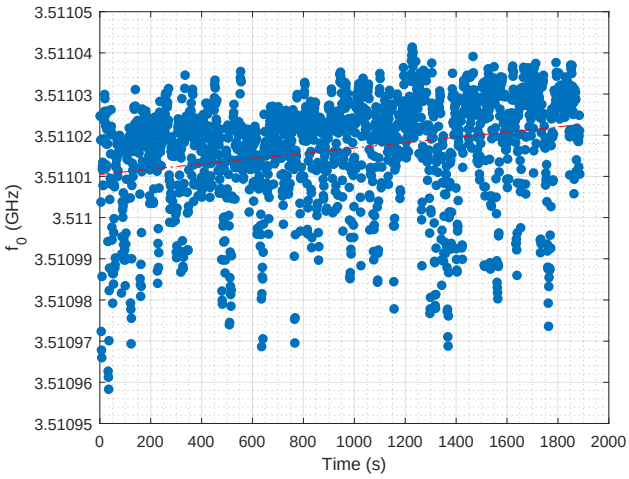

(b) The resonance frequency over time.

Figure 4.11: The cavity temperature and the resonance frequency over time with a helium gas flow.

One possible effect that can be due to the flow is a change in pressure inside the cavity. When the pressure inside the cavity changes during a pulse the relative permittivity will change as well. An analysis is made to investigate how much impact a change in pressure has on the relative permittivity of the medium and thereby on the resonance frequency. For this purpose data describing the relation between the pressure and the relative permittivity of helium has been used. The data of *F. van der Maesen* [8] and *J.W. Schmidt and M.R. Moldover* [9] are presented in Table 4.2 and shown in Figure 4.12. A linear fit is used to determine the slope of

these graphs. The value of the slope for the data of *F. van der Maesen* is $5.4 \cdot 10^{-5}$ bar^{-1} and for the data of *J.W. Schmidt and M.R. Moldover* the value of the slope is $6.0 \cdot 10^{-5}$ bar^{-1}. With these values the shift in resonance frequency is calculated for helium gas. The relation between the shift in resonance frequency and the shift in relative permittivity, $\Delta\varepsilon_r$, is given by

$$\Delta f = \frac{f_0}{2}\Delta\varepsilon_r \tag{4.12}$$

assuming that the relative permittivity is homogeneous inside the cavity and taking the real part of Equation 2.1.

Table 4.2: The relative permittivity at different values of the pressure according to F. van der Maesen [8] and J.W. Schmidt and M.R. Moldover [9].

(a) The data of F. van der Maesen [8].

Pressure (atm)	Relative permittivity
5.7	1.00043
16.91	1.00102
24.86	1.00137
33.03	1.00178
39.57	1.00217
49.5	1.00275
60.19	1.00344
64.1	1.00348
65.08	1.00377

(b) The data of J.W. Schmidt and M.R. Moldover [9].

Pressure (atm)	Relative permittivity
10.46287	1.00065
12.41964	1.00077
22.22610	1.00138
22.67673	1.00140
32.18761	1.00198
32.69183	1.00201
40.06158	1.00246
42.25097	1.00259
50.57903	1.00309
51.90081	1.00317
60.09149	1.00366
61.65685	1.00375
69.05107	1.00419

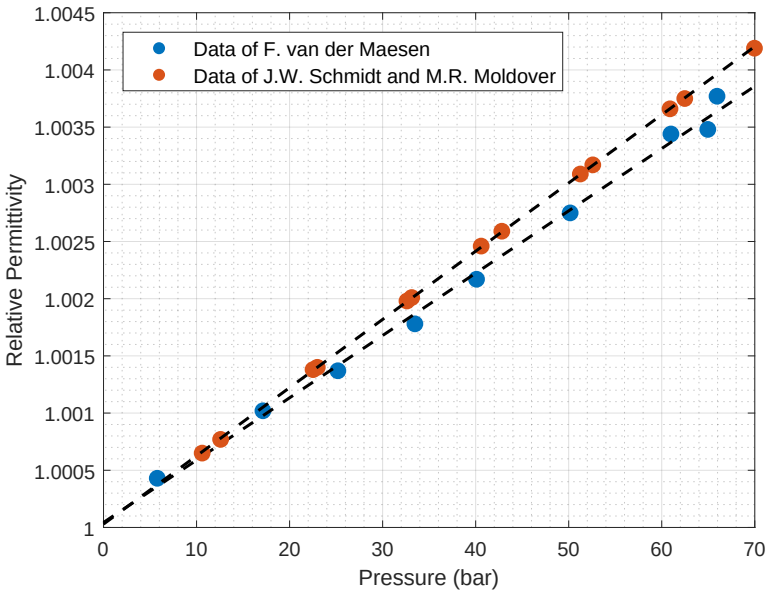

Figure 4.12: The relative permittivity plotted against the pressure for the data of F. van der Maesen [8] and J.W. Schmidt and M.R. Moldover [9].

In Figure 4.13 the shift in resonance frequency for helium gas is plotted against the change in pressure for both the data of *F. van der Maesen* and *J.W. Schmidt and M.R. Moldover* for pressure changes in the order of mbar. Pressure changes of a few mbar are plausible to occur inside the cavity. According to Figure 4.13 a noise of around 100 Hz could then be measured. This is, however, only valid in the situation that there is only helium gas inside the cavity. The relative permittivity of air is approximately ten times larger than the relative permittivity of helium and therefore pressure changes in a gas mixture of helium and air will result in a larger shift in resonance frequency than the shift obtained from Figure 4.13. However, there will probably be more movement in the helium gas flow than in the air inside the cavity. Therefore the influence of pressure changes should be experimentally determined to obtain the relation between the shift in resonance frequency and the change in pressure.

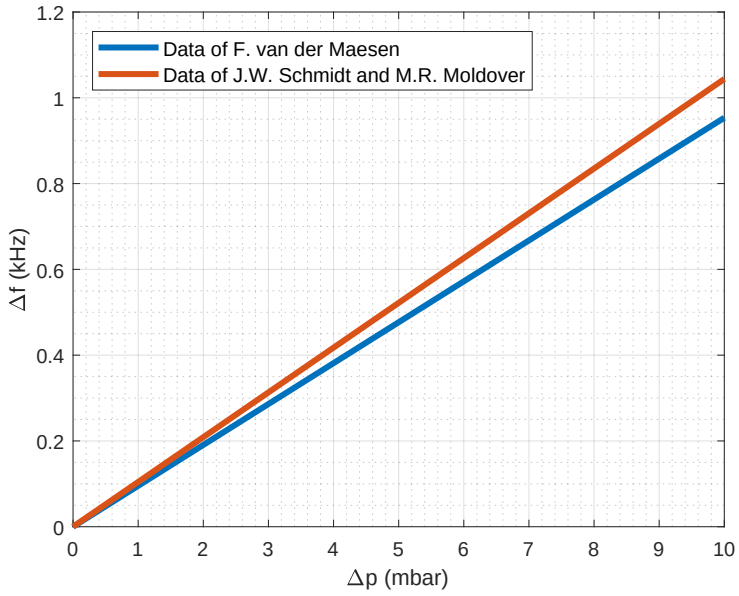

Figure 4.13: The frequency shift plotted against the change in pressure using the data of F. van der Maesen [8] and J.W. Schmidt and M.R. Moldover [9].

To determine if pressure changes in the gas flow could have caused the 70 kHz noise in Figure 4.11b, the change in resonance frequency was plotted against different pressure changes and shown in Figure 4.14. According to this figure the 70 kHz noise corresponds to a pressure change of around 670 mbar for the situation with only helium gas inside the cavity. The relative permittivity of air is 1.00059 [5], which is larger than the relative permittivity of helium that has a value of 1.0000684 [7]. Therefore the change in resonance frequency is larger too. In the case that there is only air inside the cavity the pressure change necessary for a 70 kHz noise would be 78 mbar, which is still very large since the flow was controlled with a flow controller at a constant input rate. Therefore a change in pressure is unlikely to be the cause for the noise. To confirm this hypothesis, however, the influence of pressure changes on the shift in resonance frequency should be experimentally determined.

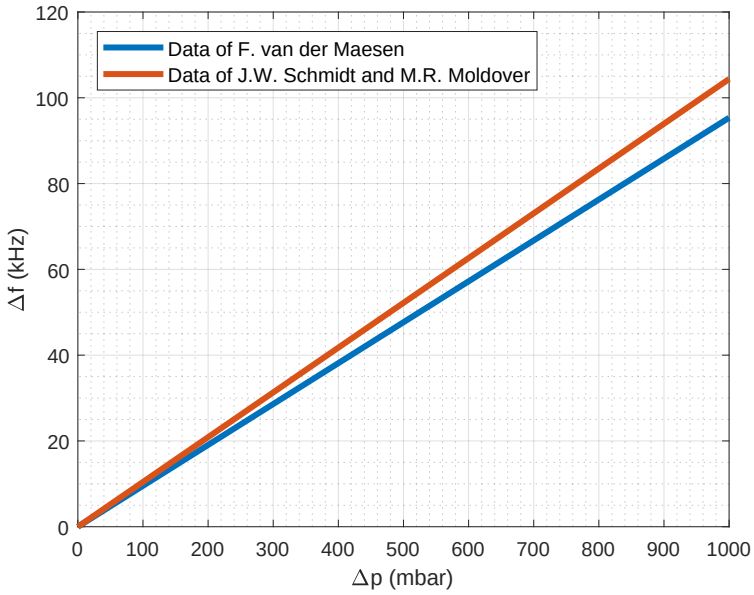

Figure 4.14: The frequency shift plotted against the change in pressure using the data of F. van der Maesen [8] and J.W. Schmidt and M.R. Moldover [9].

Another possible explanation is that the mixture of helium and air inside the cavity fluctuates. A fluctuation in the gas composition results in a different value for the relative permittivity of the medium, which in turn can be related to the resonance frequency using Equation 4.12. The relation between the change in permittivity, $\Delta\varepsilon_r$, and the percent fluctuation in the gas composition is given by

$$\Delta\varepsilon_r = \frac{\varepsilon_{r,Air} - \varepsilon_{r,He}}{50} V_{fl}, \tag{4.13}$$

where $\varepsilon_{r,Air}$ is the relative permittivity of air, $\varepsilon_{r,He}$ the relative permittivity of helium and V_{fl} the percent fluctuation in the gas composition.

By combining Equations 4.13 and 4.12 the relation between the shift in resonance frequency and the fluctuation in the gas composition can be determined and is given by

$$\Delta f = \frac{f_0(\varepsilon_{r,Air} - \varepsilon_{r,He})}{100} V_{fl}. \tag{4.14}$$

The shift in resonance frequency is plotted for different fluctuation percentages of the gas composition with $\varepsilon_{r,He} = 1.0000684$ [7] and $\varepsilon_{r,Air} = 1.00059$ [5] and is shown in Figure 4.15.

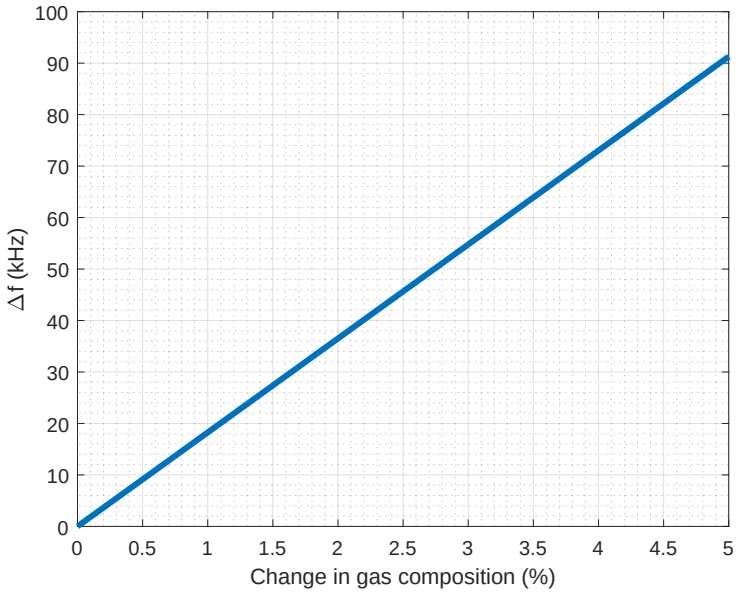

Figure 4.15: The frequency shift plotted against the change in gas composition.

According to Figure 4.15 the 70 kHz noise of Figure 4.11b corresponds to a fluctuation of the gas composition of 3.8%. Previously a fluctuation of flow around 0.5% has been measured when the setup was in a controlled environment. The environment of this measurement was not controlled and therefore the gas composition is more likely to have higher fluctuations. It is also unknown if the gas mixture reached equilibrium before the measurement started. Therefore it is plausible that the 70 kHz noise is due to the fluctuation of the gas composition. To confirm this hypothesis the measurement as described in Section 3.3 could be performed in a controlled environment to minimize the fluctuation of the gas composition or an inlet gas can be used that has the same gas composition as the surrounding gas.

Chapter 5

Conclusion

In this research three different influences are studied: the influence of the cavity temperature on the resonance frequency, the influence of the gas temperature on the cavity temperature and the influence of the helium gas flow on the resonance frequency. First the influence of the cavity temperature on the resonance frequency and the quality factor is investigated. From the results described in Section 4.1 it can be concluded that the resonance frequency changes with -73 ± 2 kHz per Kelvin increase in cavity temperature and that the quality factor decreases with increasing cavity temperature. The experimentally determined expansion coefficient of aluminum is $(20.7 \pm 0.4) \cdot 10^{-6}$ K^{-1}, which is slightly lower than the theoretical value of $24 \cdot 10^{-6}$ K^{-1}.

Secondly, the influence of the gas temperature change on the cavity temperature is investigated. For gas temperature changes between 120 and 180 K , the change in cavity temperature per pulse is in the order of 10 μK for the theoretical model and in the order of μK for the measurements. The theoretical model is above the actual change in cavity temperature, because it assumes that all the input energy is used for heating the cavity. The results of the measurements are, however, below the actual changes in cavity temperature, because some heat is lost before the gas reaches the glass tube. When a plasma is created with a plasma jet, the gas temperature increases with between 400 and 1000 K. Using the first conclusion that describes the relation between the resonance frequency and the cavity temperature, it can be concluded that in the above gas temperature range the change in resonance frequency is between the order of 1 Hz and the order of 10 Hz. From Section 4.2 it can also be concluded that lowering the duty cycle lowers the influence that the gas temperature has on the cavity temperature for a constant pulse.

Lastly, the influence of the helium gas flow on the resonance frequency is studied. The results showed a 70 kHz noise in resonance frequency with the helium gas flow compared to a 1 kHz noise in resonance frequency without flow. It is concluded that pressure changes inside the cavity due to the flow are not likely to be the cause for the 70 kHz noise, since the pressure changes would then be in the order of at least 10 mbar. Typical pressure changes are more likely to be in the order of mbar. This is, however, only a prediction since data of a cavity with only helium gas was used and therefore the influence of pressure changes on the resonance frequency should be experimentally investigated to confirm the hypothesis. Fluctuations in the gas composition can cause the 70 kHz noise. A fluctuation of 3.8% causes a shift in resonance frequency of 70 kHz, which is a plausible fluctuation. Therefore in future experiments it is important to minimize the fluctuations in the gas composition to obtain a higher resolution.

Bibliography

[1] D.B. Graves. Plasma processing. *IEEE transactions on plasma science*, 22(1), February 1994. doi: www.doi.org/10.1109/27.281547.

[2] J. Winter et al. Atmospheric pressure plasma jets: an overview of devices and new directions. *Plasma Sources Science and Technology*, 24(6), October 2015. doi: www.doi.org/10.1088/0963-0252/24/6/064001.

[3] J. Beckers et al. Thermalization of electrons in decaying extreme ultraviolet photons induced low pressure argon plasma. *Plasma Sources Science and Technology*, 25(3), April 2016. doi: www.doi.org/10.1088/0963-0252/25/3/035010.

[4] M. van der Schans et al. Decay of the electron density and the electron collision frequency between successive discharges of a pulsed plasma jet in n2. *Plasma Sources Science and Technology*, 28(3), March 2019. doi: www.doi.org/10.1088/1361-6595/ab096e.

[5] R.A. Freedman H.D. Young. *University Physics with Modern Physics*. Pearson Education, 14th global edition, 2016.

[6] J.T. Padding M. van Sint Annaland, J.A.M. Kuipers. *Lecture notes Fysische Transport Verschijnselen*. Department of Chemical Engineering and Chemistry, Eindhoven University of Technology, April 2017.

[7] D.R. Lide. *CRC Handbook of Chemistry and Physics*. CRC Press, internet version edition, 2005.

[8] F. van der Maesen. *De absolute dielectrische constante van gassen*. University of Amsterdam, February 1950.

[9] M.R. Moldover J.W. Schmidt. Dielectric permittivity of eight gases measured with cross capacitors. *International Journal of Thermophysics*, 24(2), March 2003. doi: www.doi.org/10.1023/A:1022963720063.

Appendix A

Results of the gas heating experiment

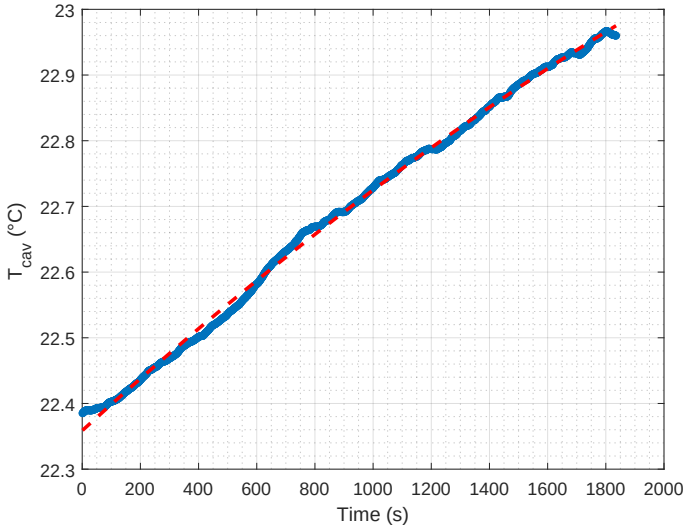

(a) The cavity temperature over time for $T_{gas} = 120\ ^{\circ}C$.

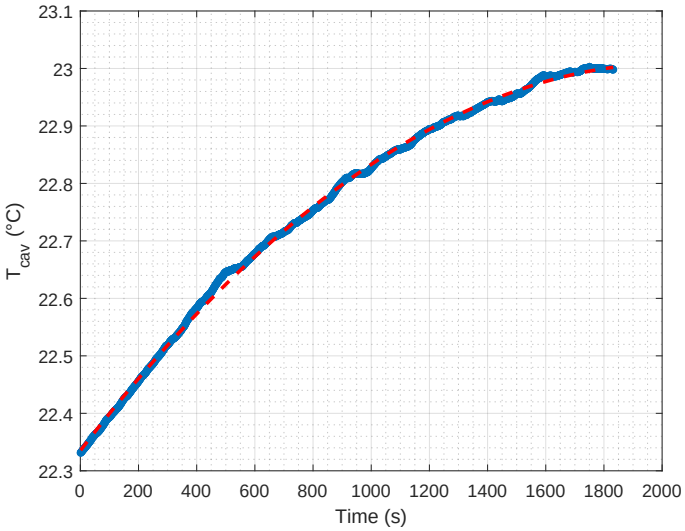

(b) The cavity temperature over time for $T_{gas} = 130\ ^{\circ}C$.

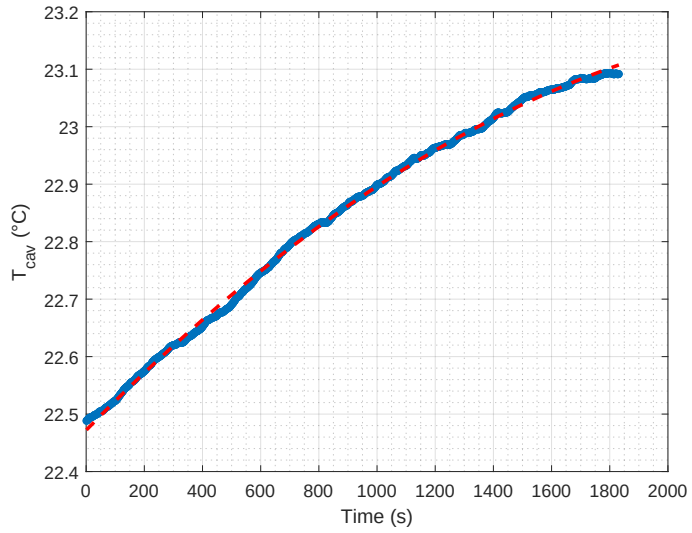

(c) The cavity temperature over time for $T_{gas} = 140\ ^{\circ}C$.

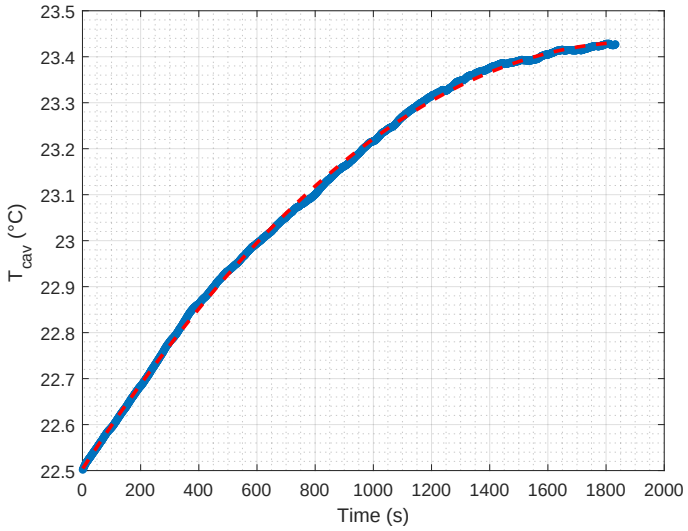

(d) The cavity temperature over time for $T_{gas} = 150\ ^{\circ}C$.

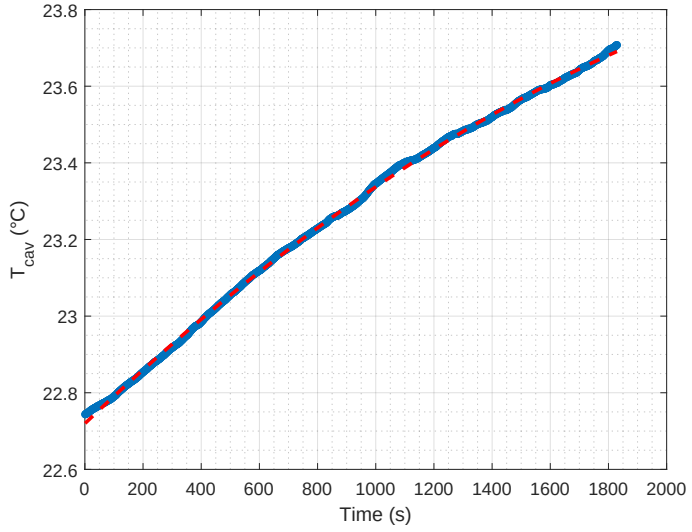

(e) The cavity temperature over time for $T_{gas} = 160\ ^{\circ}C$.

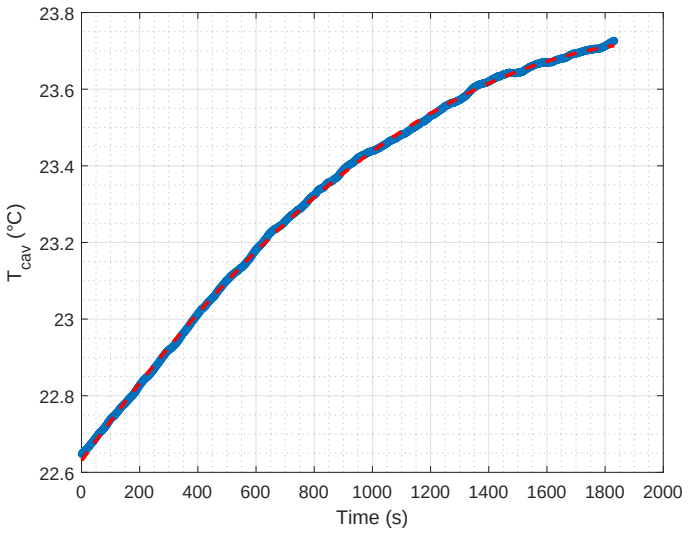

(f) The cavity temperature over time for $T_{gas} = 170\ ^{\circ}C$.

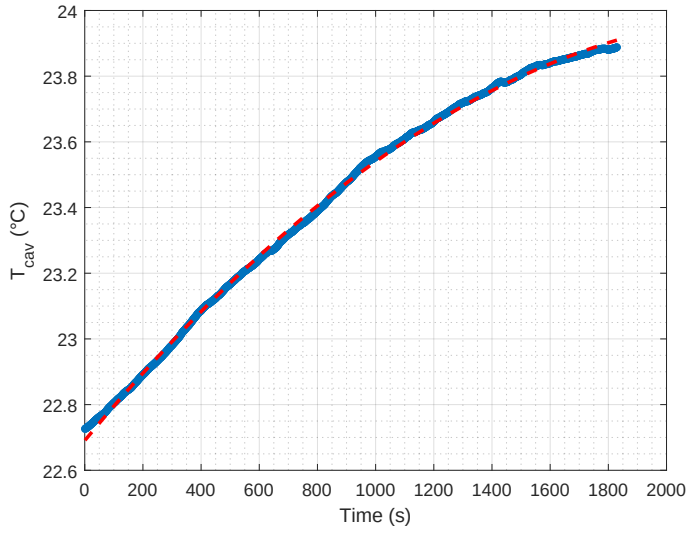

(g) The cavity temperature over time for $T_{gas} = 180\ ^{\circ}C$.

Figure A.1: The cavity temperature over time for different gas temperatures with a second degree polynomial fit.